The FLUKA Monte Carlo Simulation of the magnetic spectrometer of the FOOT experiment

Y. Dong[a,*], S.M. Valle[f,1], G. Battistoni[a], I. Mattei[a], S. Muraro[a], C. Finck[d], V. Patera[c,e], and the FOOT Collaboration

[a] *INFN Sezione di Milano, via Celoria 16, 20133 Milano, Italy*
[b] *S.S. Lazio, Roma, Italy*
[c] *Dipartimento di Scienze di Base ed Applicate dell'Università di Roma, "La Sapienza",Italy*
[d] *Université de Strasbourg, CNRS, IPHC UMR 7871, Strasbourg, France*
[e] *INFN Sezione di Roma, Italy*
[f] *Istituto Tecnico Agrario Statale "Carlo Gallini", Voghera (Pv), Italy*

Abstract

The FOOT experiment of INFN is devoted to the measurement of the nuclear fragmentation double differential cross sections useful for the improvement of calculation models adopted in hadrontherapy and radioprotection. A detailed Monte Carlo simulation of the FOOT magnetic spectrometer has been implemented in order to optimize the design and to guide data analysis. This task has been accomplished by means of the FLUKA Monte Carlo code. The input files of the FLUKA simulations are generated within the software framework of the experiment, in order to have a consistent generation and description of geometry and materials in both simulation and data analysis. In addition, this assures the possibility of processing both simulated and real experimental data with the same data analysis procedures. Databases containing specific parameters describing the setup employed in each different experimental campaign are used. A customized event-by-event output of the Monte Carlo code has been developed. It can be readout by the general software framework of FOOT, enabling the access to the generation history of all particles in the same event. This output structure therefore gives the possibility to perform a detailed analysis and study of all relevant processes, allowing the detailed tracking reconstruction of all individual particles. Examples of results are presented.

Keywords: Nuclear Physics, Monte Carlo, Particle Detectors

1. Introduction

Nuclear fragmentation processes induced by hadrons and nuclei interacting with matter are of great interest not only in fundamental research but also in applied physics, as for example in Charged Particle Therapy (CPT) and Radiation Protection in Space (RPS). Indeed, nuclear fragmentation processes have a significant impact on the computing of both physical and biologically effective dose.

In CPT, the characteristic distribution of energy deposition of ionized nuclei (Bragg peak), as well as their high Relative Biological Effectiveness (RBE), is exploited to treat deep-seated tumors with high spatial selectivity. Nuclear fragmentation of both target and beam nuclei affects the planned dose distribution and consequently, in order to guarantee the treatment quality, these processes have to be carefully taken into account[1, 2]. Target fragmentation may be relevant especially in proton therapy since secondary fragments, although having a very small range, have a significantly higher RBE with respect to primary protons. At

*Corresponding author
Email address: yunsheng.dong@mi.infn.it (Y. Dong)
[1] Before 2021 at INFN Milano

present, target fragmentation induced by proton beams impinging on human tissues nuclei is often neglected in dose calculation [3, 4].

In RPS the development of shields effective at preserving spacecraft crew members from ionizing space radiation is a crucial item. Especially in long duration and far form Earth space missions the integral dose received by the astronauts is a serious health hazard. Nuclear fragmentation induced by the interaction of the high energy space radiation and the shield nuclei leads to the production of light and highly penetrating radiation that must be taken into account in shielding design [5, 6, 7, 8].

The total and differential cross sections related to fragmentation processes are needed for the calculation of fragments production and a correct estimation of the dose. This knowledge is necessary to correctly develop treatment plans and assess the health risk in space missions. At present, these cross sections in the energy range of interest for CPT (from few tens of MeV/u up to about 400 MeV/u) and for RPS applications (several hundreds of MeV/u and above) are not fully covered by experimental measurements. Such data would be fundamental for the improvement of the calculation models adopted in Monte Carlo (MC) codes. Currently, MC simulations are considered as the best tool to calculate the contribution of secondary fragments for many applications, including particle therapy and radioprotection[9, 10]. However, the nuclear models embedded in MC codes do not derive from exact calculable theories but have a phenomenological character. Consequently they suffer from many uncertainties[2]. To increase their reliability these models have to be continuously improved and benchmarked with experimental data[11].

The FOOT (FragmentatiOn Of Target) experiment aims to experimentally measure double differential cross sections for fragments production for energies, beams and targets of relevance for CPT and RPS. The experimental program includes the study of the fragmentation induced by proton, ^{4}He, ^{12}C and ^{16}O beams in targets composed of the most abundant nuclei in the human body (H, C and O)[12].

In order to optimize the detectors layout and to study the detector performances in identifying the fragments and in measuring energy and direction, a detailed simulation has been developed. The FOOT simulation is based on the FLUKA simulation code[13, 14, 15, 16] and is integrated into the FOOT software framework SHOE (*Software for Hadrontherapy Optimization Experiment*).

In this work, we are going to review the status of all the components and procedures adopted for the simulation of the FOOT magnetic spectrometer. We will first describe how the geometry is constructed and managed. A customized event-by-event output has been constructed, enabling to perform a detailed analysis of each event with the possibility of accessing the generation history of all particles depositing energy in each sub-detector. Examples of results will be presented.

The FOOT apparatus will be briefly described in Section 2. The generalities about the FLUKA code and its customized use for FOOT experiment are then summarized in Section 3. In Section 4 the interface procedures to manage the simulation runs, built within the software framework of the experiment, are illustrated. Examples of simulation results are then shown in Section 5.

2. The FOOT experiment

2.1. Aims, strategies and research program

FOOT is an experiment funded by Italian National Institute for Nuclear Physics (INFN) and aims to measure double differential cross section of fragments production with the resolution that matches the desiderata of

radiobiologists in view of the development of improved Treatment Planning Systems. The fragmentation of ^{4}He, ^{12}C and ^{16}O beams will be studied at therapeutic energies (200 MeV/u $\sim$ 400 MeV/u) as well as at higher energies ($\sim$ 800 MeV/u) of interest in RPS. The target composition has to be representative of the human body tissue, whose major components are Carbon, Oxygen and Hydrogen. Different targets will be therefore used: graphite (C), polyethylene (C_2H_4) and PMMA ($C_5O_2H_8$). Since these materials are compounds of C, O and H, cross sections on these elements will be obtained by subtraction [17, 18]. Given the variety of particles and energy required for the incident beam, the experimental program is conducted at different hadron therapy centers and facilities with particle accelerators, e.g.: CNAO National Center for Oncological Hadrontherapy (Pavia, Italy), GSI Helmholtz Centre for Heavy Ion Research (Darmstadt, Germany) and HIT Heidelberg Ion Beam Therapy Center (Heidelberg, Germany). Due to the necessity to relocate the entire experimental setup at each data taking campaign, the apparatus has been designed as a table-top experiment.

The most challenging goal of FOOT is to measure the fragments production induced by a proton beam at therapeutic energy ($\sim$ 200 MeV). Due to kinematic reasons, target fragments have very low energy and short range (few tens or hundreds of µm) and their detection is extremely tough. Therefore an inverse kinematic approach will be adopted in FOOT: the target fragmentation cross sections for protons on C and O will be obtained by inverting the kinematics of the reconstructed fragmentation events of ^{12}C and ^{16}O on hydrogen enriched targets (as before, polyethylene and PMMA) and inverting the reaction kinematics through the application of the Lorentz transformations [12].

To measure the cross sections, the identification of atomic number (Z) and atomic mass (A) of all secondary fragments is crucial as well as the measurement of their energy and angular spectra. The stringent requirements in terms of resolution of the measurements together with the need of portability of the detector have driven the choice and the design of the detector setup. Since FOOT has been designed to be a fixed target experiment, the chosen solution that fulfills these requirements is a magnetic spectrometer, composed of a permanent magnet and high precision tracking detectors, coupled with other detectors for particle identification. Preliminary simulations have been performed to drive the design of the experimental setup. These studies, together with the results of a previous experiment[19], have shown that for projectiles like ^{16}O and ^{12}C at the energies of interest (200 MeV/u or higher) the angular distribution of secondary fragments narrows as the charge and mass increases: heavier ($Z > 2$) fragments are forward peaked within a polar angle of $\sim 10°$, while lighter ($Z \leq 2$) fragments are emitted also at larger angles. Due to the large angular aperture of the $Z \leq 2$ fragments, the needed size, weight and cost of a wide angle magnetic spectrometer would have not be affordable. Two different experimental setups have been considered: an Magnetic Spectrometer (MS), optimized for heavier ($Z \geq 3$) fragments, and an Emulsion Cloud Chamber (ECC) spectrometer dedicated to the measurement of lighter ($Z \leq 3$) fragments. A detailed description of the FOOT experiment has been published elsewhere[12]. Here we summarize the description of the MS, since it is the relevant case for the simulation code object of the present article.

2.2. The FOOT setup

Three different regions can be identified in the apparatus shown in Fig. 1. For a more detailed description see 3.3.

- In the *pre-target region* a Start Counter (SC) and a Beam Monitor (BM) are placed before the target and are used to monitor the beam parameters. The SC is a plastic scintillator adopted to measure the rate of

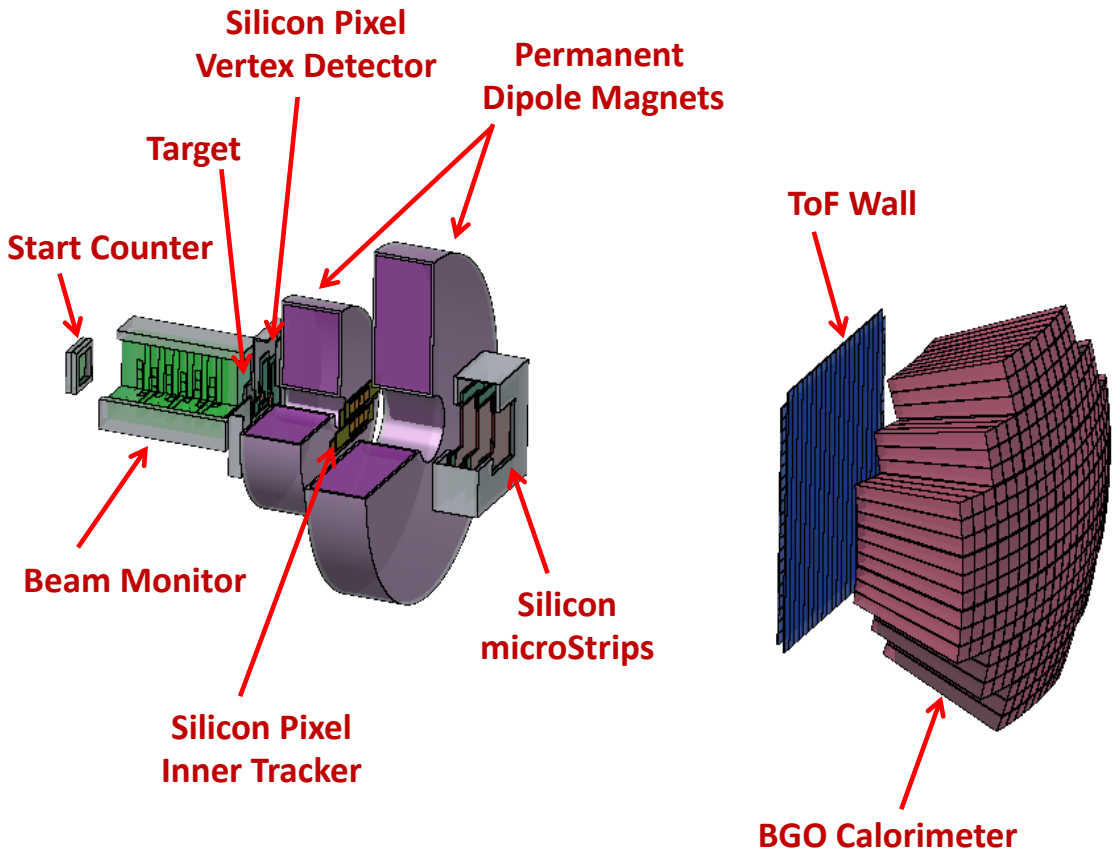

Figure 1: A schematic representation of the FOOT magnetic spectrometer setup as obtained by the geometry visualizer of the FLUKA code

primaries, to provide the trigger signal for event and to mark the start time of the Time Of Flight (TOF) measurement. The BM is a drift chamber placed between the SC and the target. This detector is adopted to measure the projectile direction and impinging position on the target. The trajectory of the primary particle is required for the application of the Lorentz transformation necessary for the kinematic inversion adopted in the target fragmentation measurements. The projectile impinging point is adopted to identify the particle interaction point within the target, which is useful for matching the reconstructed fragment tracks. The spatial resolution of the BM has been found to be of the order of hundreds of μm [20].

- The tracking system providing the measurement of momentum includes two cylindrical permanent magnets and three precision tracking stations. The two Permanent Magnets (PMs) are designed in the Halbach configuration providing an approximately dipolar magnetic field within the internal bores. The maximum magnetic field is $\sim 1.4\,\mathrm{T}$. The tracking detectors are placed before, between and beyond the two PMs. They are composed of different layers of silicon CMOS pixel and silicon microstrip detectors, aiming to reconstruct the Z$\geq$ 3 fragments tracks and momentum with a momentum resolution of about $\sim 5\%$.

- The *downstream region* includes two detector systems developed for the charge identification and kinetic energy measurement tasks. A Tof Wall (TW) detector composed of two layers of plastic scintillator bars is adopted for the measurement of the energy loss ΔE of fragments and, together with the SC, the TOF

with a resolution of the order of 70-80 *ps* for $Z > 2$ fragment. Both measurements are used to perform the charge identification with a precision of the order of few percent [21]. The kinetic energy E_{kin} of the fragments is measured with a $Bi_4Ge_3O_{12}$ (BGO) crystal calorimeter which has an energy resolution of the order of few percents. The isotope identification can be performed combining the momentum, TOF and kinetic energy measurements.

3. The FLUKA simulation of the FOOT experiment

The FOOT simulation has been built in the framework of the general purpose, condensed history MC code FLUKA MC code[13, 14]. FLUKA is a theory driven MC code, based on original and extensively tested microscopic models which consider the basic constituents of matter. The microscopic approach ensures the fulfilling of conservation laws and provides the proper correlations among the interaction products. FLUKA models have been extensively benchmarked with experimental data at single interaction level using a limited number of free parameters, which are fixed for all energies, targets and projectiles. Interested readers can find extensive descriptions of the physics content and technical features of FLUKA in several specific references [13, 14, 22, 23, 24, 16, 25, 26].

At the energies relevant for the FOOT experiment, the main physics models of interest concern the propagation in the nucleus of the hadrons involved in elementary multiple collisions. This is simulated through a Generalized Intra Nuclear Cascade model GINC included in the PEANUT (PreEquilibrium Approach to NUclear Thermalization) package of FLUKA, which also manages the *pre-equilibrium emission* stage. At energies below 125 MeV, the nucleus-nucleus interactions are managed by the Boltzman Master Equation BME model [24] and, for energy lower than 5 GeV, by a modified version of the relativistic Quantum Molecular Dynamics model rQMD-2.4 [27, 28, 29].

In the following paragraphs we shall summarize the basic concepts used to construct the input and the geometry of FLUKA and the specific attentions required in FOOT: the handling of the magnetic field and the construction of the required customized output by means of user routines.

3.1. Standard input and geometry

All the directives for a FLUKA simulation are provided by the user by means of a series of commands, often called *data cards*, listed in an input ASCII file. Several numerical parameters can be passed to the code using the cards. In this way, it is possible to define the primary beam, the number of required histories, transport and generation thresholds, physics settings, a number of pre-defined scoring options, the definition and elemental composition of materials. Either in the same input file (with `.inp` extension), or in a separated one (usually, but not necessarily, with `.geo` extension), also the geometry of the simulation can be constructed by means of a data card listing. Details on the construction of the geometry of the FOOT apparatus are given in sec.3.3.

3.2. Default settings and Energy Thresholds

The FLUKA code has a number of pre-defined sets of physics parameter settings, passed in the input file through the card `DEFAULTS`. We have chosen to adopt the `PRECISIO` default, which is recommended for precision simulations. In particular, the `PRECISIO` physics settings include the activation of all models and set a charged particle and photon transport minimum threshold at 100 keV, while for neutrons is set at 10 µeV.

The use of a low energy threshold for photons and electrons requires however some discussion. The case of electrons is particularly relevant, since a low energy cut-off for e^+e^-, as it could be required to consider δ-ray production and transport, may lead to very long computing times and very large event-by-event output files (see Sec.5.1). Instead, photon energy threshold has much less impact on computing time, due to the obvious differences in transport and interactions. Therefore, a careful study has been carried out about the effect of considering different values for e^+e^- cut-off and the explicit production of δ-rays. It turned out that, in the case of FOOT, from the point of view of the integrated energy deposition on each detector, the carefully tuned models of FLUKA managing dE/dx fluctuations guarantee a result which is independent of the choice of the e^+e^- cut-off value. The explicit production and transport of electrons may instead, in some cases, affect the spatial distribution of the energy deposition. This can be relevant mostly for the gaseous detector and the silicon pixel sensors. However, in both cases, it turned out that it is possible to perform the simulations maintaining the reliability without an explicit δ-ray production. For the Beam Monitor, signals from δ-rays can be suppressed during experimental data takings setting a proper threshold in the readout electronics. In addition, δ-rays and other background effects can be generated and added to the MC simulation output during the data reconstruction and analysis phase. In the case of silicon sensors, δ-ray effects can be considered by the inclusion of a pixel clustering algorithm during the reconstruction of simulated depositions in the silicon sensors. This is achieved by considering a parametrization of cluster size as a function of energy deposition derived from the analysis of experimental data. In this case, the inclusion of δ-rays would introduce a double counting.

Hence, we kept the particle transport thresholds of the `PRECISIO` default for hadrons and muons, but we switched off the transport of e^+e^- by raising up their energy cut-off to a large value (1 GeV), in all simulations devoted to the understanding of the nuclear fraction detection. In other particular cases, these threshold were restored to values in the range 10-100 keV, according to the specific purposes of the simulation runs. The production and transport threshold for photons can be instead easily kept low enough in order to account for all relevant processes, including nuclear de-excitation, positron annihilation etc.

3.3. FOOT input geometry

In the geometry of the FOOT MS implemented in FLUKA, the center of the target has been chosen as the origin of the global Cartesian reference frame. The z axis is chosen as the beam axis. The relative position of all detectors is variable and depends on the specific experimental campaign in a given facility. For instance, the distance between the target and the downstream region detectors (TW and calorimeter) can be increased when taking data at higher energies in order to improve the β resolution for a given TOF resolution, at the price of decreasing the geometrical acceptance.

All FOOT geometrical elements represented in Fig.1 have been implemented using the high accuracy option of FLUKA geometry, which allows up to 16 significant digits. The description of materials in terms of elemental composition was carefully considered. Whenever possible, such as in the case of plastic scintillators, data sheets provided by manufacturers, were used as references.

Beyond active detectors, some care has been taken to consider also those passive elements which can be relevant for re-interactions of secondaries generated in target and produce background. In the following, we shall summarize the essential details considered in the simulated geometry of each detector.

- the Start Counter is simulated as a 250 µm thick plastic scintillator coated with two 10 μm thick Mylar layers, enclosed in an aluminum frame and placed perpendicularly with respect to the beam axis. The

detector has a sensitive area of 7 cm × 7 cm, but the squared holes in the aluminum frame is of 5 cm × 5 cm (Fig. 2);

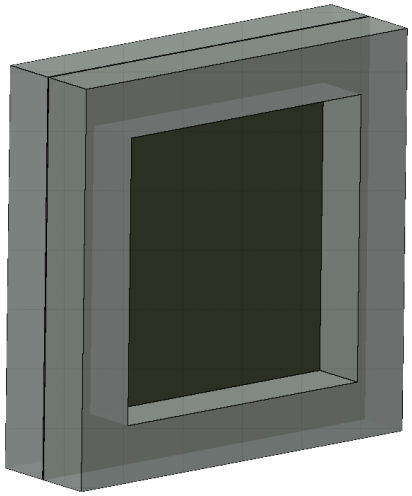

Figure 2: 3D rendering of simulated SC

- the Beam Monitor is filled with a Ar/CO_2 80/20% gas mixture and it is made of 12 planes of alternated horizontal and vertical drift cells. Each plane has 3 rectangular cells (16 mm × 10 mm). In each view, two consecutive layers are staggered by half a cell to solve left-right ambiguities in track reconstruction. The total size of the chamber is 11 cm × 11 cm × 21 cm. This detector is simulated as a parallelepiped filled with gas, surrounded by an aluminum box. The aluminum container and the mylar entrance and exit windows are also simulated. Fictitious parallelepiped regions of gas simulating the cells have also been added: in this way the scoring can be performed only in the cells and not in the entire gas region, thus saving computing time and memory. Both the anode and the cathode wires have been implemented as well, since primary particles have a non null probability of interacting with them. (Fig. 3);

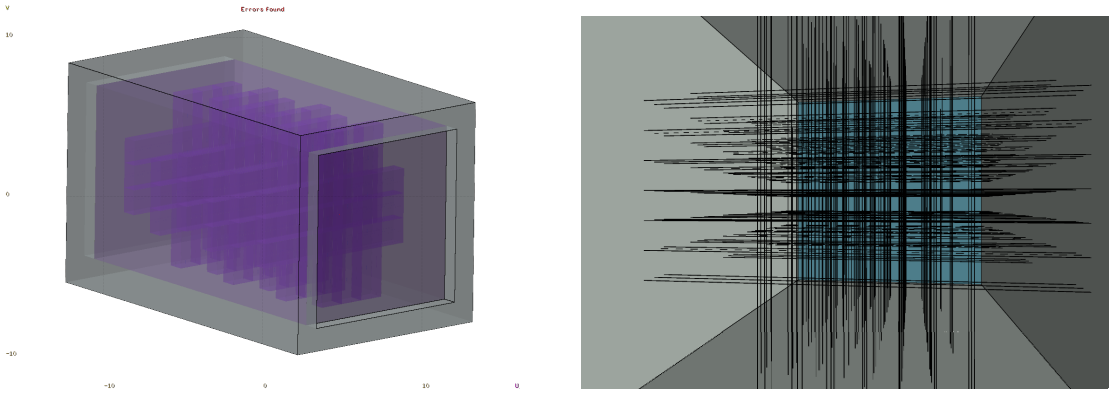

(a) (b)

Figure 3: (a) 3D view of the simulated BM; the cells structure is visible. (b) Internal view of BM showing the net of cathode and anode wires

- the target and Vertex detector (VT) region is shown in Fig.4. The target is simulated as a simple parallelepiped, made of the desired material: usually graphite or polyethylene. Due to the particular relevance, in simulation we adopt the measured density of the employed target materials. The VT detector

is a stack of four MIMOSA28 (M28) [30] silicon chips placed right after the target and before the first PM. Each sensor is a matrix of 928 rows×60 columns of pixels, 20.7 µm pitch, for a total sensitive volume of 20.22 mm × 22.71 mm × 50 µm. The VT layers are simulated considering also the printed circuit board where the pixel sensors have been mounted according to the real M28 design. The sensitive region in each VT sensor has a thickness which corresponds to the depth of the M28 epitaxial layer, and is bordered by an insensitive silicon frame region. To avoid the implementation of an excessive number of regions, the individual pixels are not simulated in the geometry. Instead, starting from the hit position, a specific algorithm coded in the user routines calculates run-time the row and column corresponding to the hit pixel. Then, this information is saved in the output file. In addition, also the aluminum box containing the VT frames is simulated.

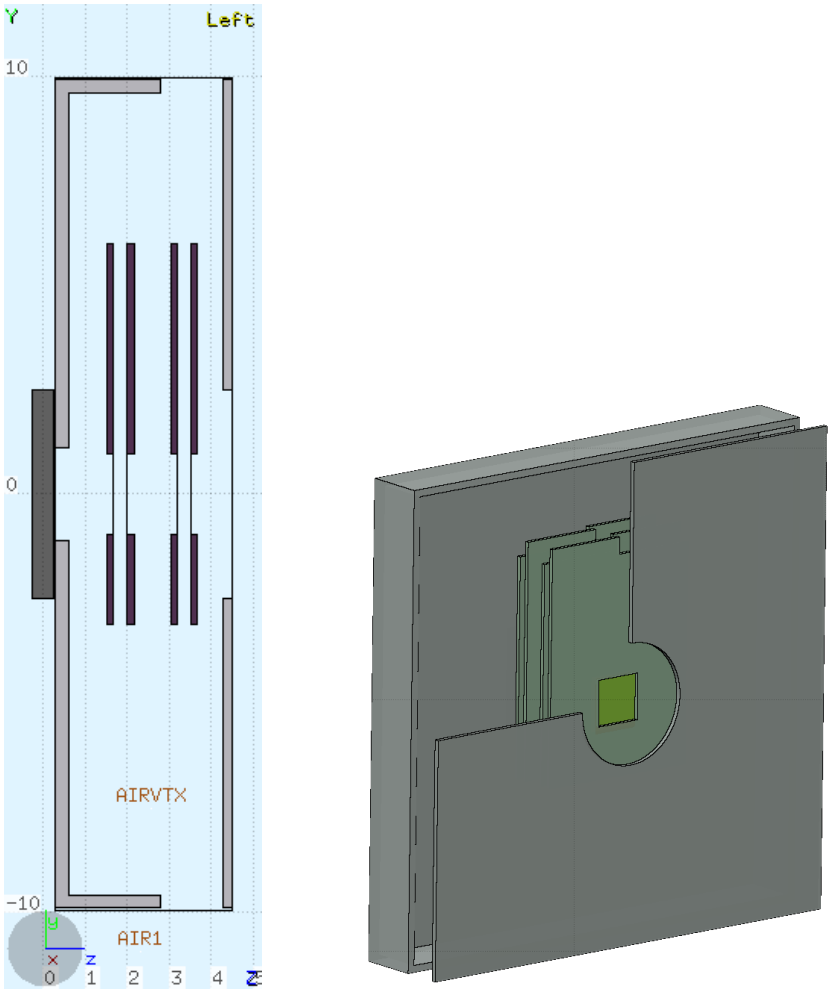

(a) (b)

Figure 4: (a) $y - z$ view showing a graphite target, 5 mm thick, and the four VT planes. (b) 3D view of the VT box. The cut allows to visualize the simulated printed circuit boards and the silicon pixel sensor

- the two permanent dipole magnets (DI) in the Halbach configuration are simulated as annular magnets made of a Nd-Fe-B mixture, surrounded by a 5 mm thick aluminum case, according to the construction design (Fig. 5). The upstream magnet has a bore diameter of 5 cm, while the downstream magnet has a larger aperture, 10.6 cm, so to achieve the required angular acceptance for the fragments produced in target. Since the magnets are only passive elements, the blocks composing each magnet have been

neglected for simplicity, and the DI are simulated as homogeneous rings. The inclusion of the magnetic

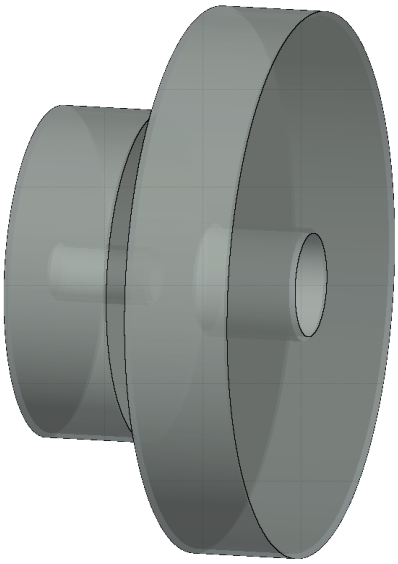

Figure 5: 3D rendering of simulated magnet bodies

field generated by these dipoles is discussed in Section 3.5.

- The second tracking station, the Inner Tracker (IT), is placed between the two PMs and it is composed of 32 M28 chips, but in this case disposed in two layers ladders in order to cover a larger area according to the enlarging spatial distribution of the fragments as they get far from the target. The M28 chips integrated in the four IT ladders are simulated exactly as the VT planes. In addition, the various passive layers composing each ladder have been implemented with the correct material assignment (Fig. 6). Thus, all the effects due to the ladder materials are simulated too, considering both MCS and background generation;

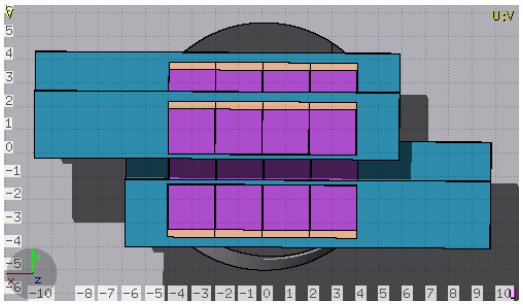

Figure 6: Visualization of the IT simulated geometry, showing the 4 interleaved ladders. Each ladder has 4 M28 sensors on one side and 4 corresponding sensors on the other.

- The Microstrip Silicon Detector (MSD) is the final tracking station (Fig.7). This detector is a telescope composed of three double layers of single sided silicon detector sensors (X-Y oriented strips for each double layer) glued on a hybrid Printed Circuit Board (PCB) and placed beyond the second PM. Each strip layer is composed of 640 strips that have a total active area of 9.6 cm × 9.6 cm. Each strip has a pitch of 50 µm with a thickness of 150 µm. Similarly to pixels, the sensitive (epitaxial) layer, the passive silicon volume and the aluminum cage is reproduced in the simulation. Also in this case we have not implemented the

individual microstrips as separate regions in the geometry: they are instead retrieved during the simulation run by a specific algorithm in the user routines.

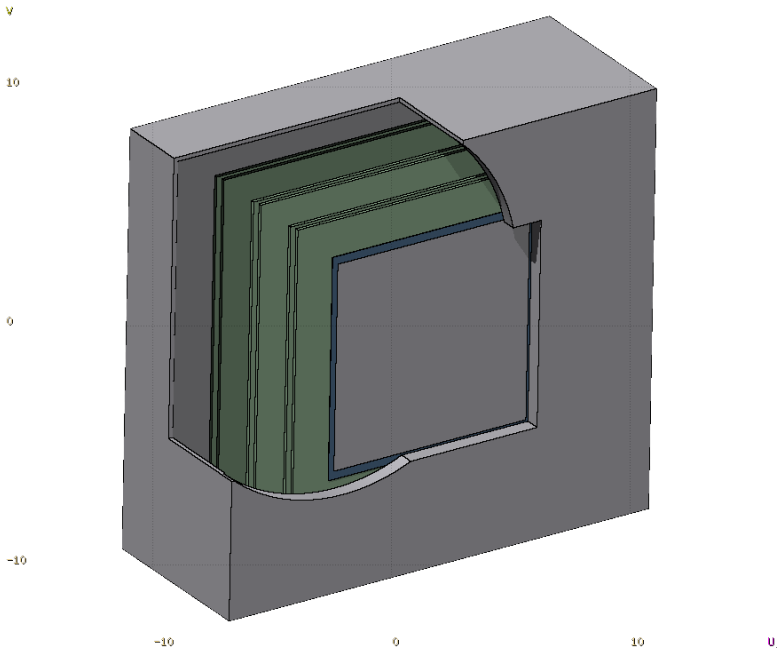

Figure 7: 3D rendering of the MSD detector box. The cut in the box allows to visualize the 6 printed circuit boards with the silicon strip sensor.

The TW is made of two layers of plastic scintillator bars, 2 mm thick and with an area of 40 cm × 2 cm, orthogonally oriented, so to provide a square scintillator wall of 40 cm × 40 cm area. The calorimeter is composed of 320 BGO crystals arranged in a spherical configuration. Each crystal is a truncated pyramid with a length of 24 cm and the two bases with an area of 2 cm × 2 cm and 3 cm × 3 cm. Unlike pixels and microstrips, both the TW (Fig. 8) and the calorimeter (Fig. 9) segmentation are reproduced in the geometry file. The truncated pyramid has become a standard FLUKA body only in the most recent version of the code. Due to the complex orientation of the different crystals, we have preferred to implement the truncated pyramid as regions delimited by 6 oriented planes. For both TW and calorimeter, we have not included in simulation any passive material, such as the box containing the calorimeter and the wrapping of TW bars and BGO crystals.

3.4. Primary Beam

Primary particles are simulated as a beam along the z direction. The injection point of the primary is set at an upstream distance corresponding to the distance between the beam nozzle and the SC, measured during the data taking. In this way, the energy loss in air of primary in the trajectory between the beam exit window and the SC is taken into account.

As far as the transverse structure of the beam is concerned, it is important to reproduce the real situation of the beam in each data taking campaign. For this purpose, the standard approach is to have a 2-dimensional Gaussian approximation, using as FWHM in the x and y coordinates the values measured by the beam monitoring devices existing in the experimental facilities where the experiment takes place. The two transverse coordinates are in general considered as independent. However, if required, it is also possible to consider more complex shapes, or introduce correlations and emittance effects, by means of specific sampling routines.

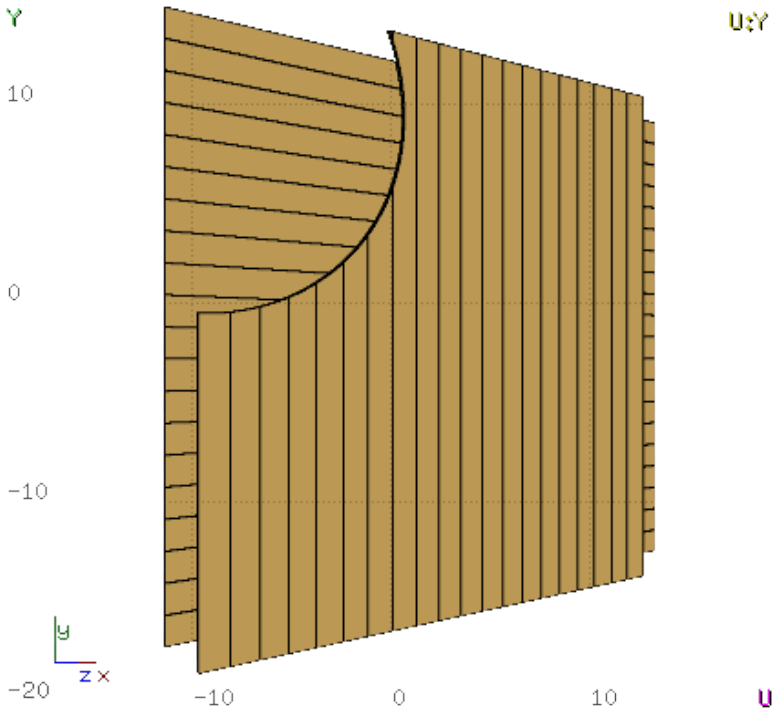

Figure 8: 3D view of the TW detector, showing the scintillator bar structure of the front and rear layers.

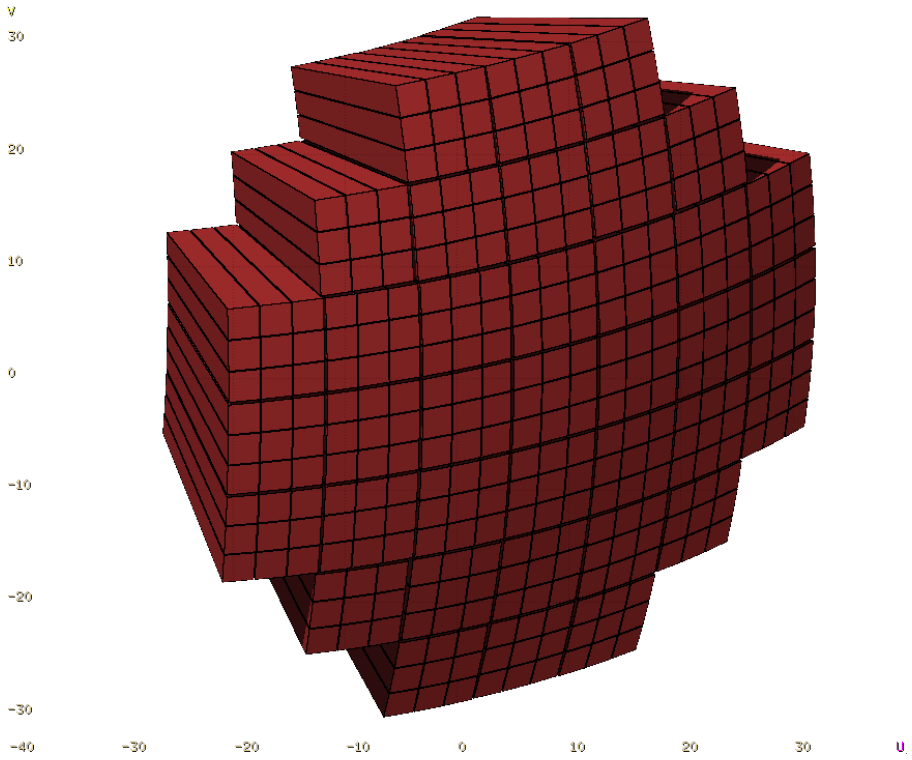

Figure 9: 3D view of the BGO calorimeter. The assembly structure, made of 3x3 crystal modules, is visible.

3.5. Magnetic field

Simulation studies were fundamental to evaluate the resolution in momentum that the FOOT MS can achieve by means of the measurement of the curvature of charged particles in magnetic field. The dipolar field provided by the two permanent magnets is not uniform. Therefore, both the simulation code and the reconstruction software obtain the values of the $\vec{B}$ field components by means of an interpolation of a 3D map. Such a map

consists of an ASCII file reporting in a table the three components of the field in a 3D mesh of points evenly spaced by 0.5 cm along each direction. The field map is provided for a region of space which extends along the beam axis, z, for $\pm$50 cm from the center of the two dipole system, while the lateral size, in the x-y view, is 10 cm wide (the size of the largest bore of the two magnets). Such extension is sufficient to account for the fringe field outside the magnets. A dedicated user routine is used in FLUKA to read the map at initialization time and return at run time the components of the magnetic field vector in any point by means of a standard trilinear interpolation method (*i.e.* a linear interpolation o a 3-dimensional regular grid, equivalent to a B-spline interpolation of order 1). Hence, at each particle step, the code can retrieve the magnetic field acting on that particle in that precise point. The simulation has been defined using the calculated map, as provided by the producer by means of the OPERA-3D design code[31]. However, the magnetic field has been experimentally measured in a similar grid of space points. Once the experimental map will be available, the magnetic map adopted in the simulation will be updated.

Fig. 10 shows the 2D field map in the region of space where tracking in magnetic field is relevant, together with the plot of the magnitude of magnetic field vector as a function of the beam axis coordinate.

In FLUKA the tracking of charged particles in magnetic field requires the setting of some parameters concerning tracking accuracy. The transport in magnetic field inside materials involves the combination of angular deflections due to the magnetic field and the multiple scattering. The usual approximation used in the condensed history approach, consisting in applying the cumulative effect of multiple Coulomb scattering over the step length at the end of the step, is unavoidably inexact. In order to achieve the required accuracy, it is necessary to force the minimum step length in particle tracking to be comparable to the minimum dimensions of the regions where magnetic field is relevant. In the case of gases (the air regions in our simulation) this issue is of particular importance also for large volumes. Then, the use of very thin detectors (∼tens or hundreds of µm) as the 50 µm thick pixel detectors (VT and IT), or the 150 µm thick silicon microstrips (MSD), necessarily demands the optimization of minimum step length. FLUKA allows to set some parameters when tracking in magnetic field is invoked. Typically:

1. the largest angle in degrees that a charged particle is allowed to travel in a single step;
2. the minimum accuracy accepted in determining the intersection with a region boundary;
3. the minimum step length if the step is forced to be smaller because the angle is larger than the limit determined by the first parameter.

The default values of these parameters usually allow to treat the majority of the situations. However, the default value of 0.05 cm for the minimum step length turned out to be insufficient. Several solutions have been tested and an accuracy of 0.1 µm for the minimum step length and 0.1° for the maximum angle in the VT, IT and MSD regions provided a suitable tracking accuracy and a sustainable CPU time usage (see sec. 5.1). A 10 µm minimum step was adopted for the air region. The use of a small step is also important in regions where a significant gradient of the $\vec{B}$-field exists.

3.6. FOOT Customized Output and user routines

The FOOT experiment requires a customized event-by-event output since simulated data have to be processed as real experimental data. This is not a standard in FLUKA, but it can be obtained by programming a set of user routines which allow to to perform high level operations in different stages of the simulation process. The different detectors composing the FOOT experimental setup provide different types of information.

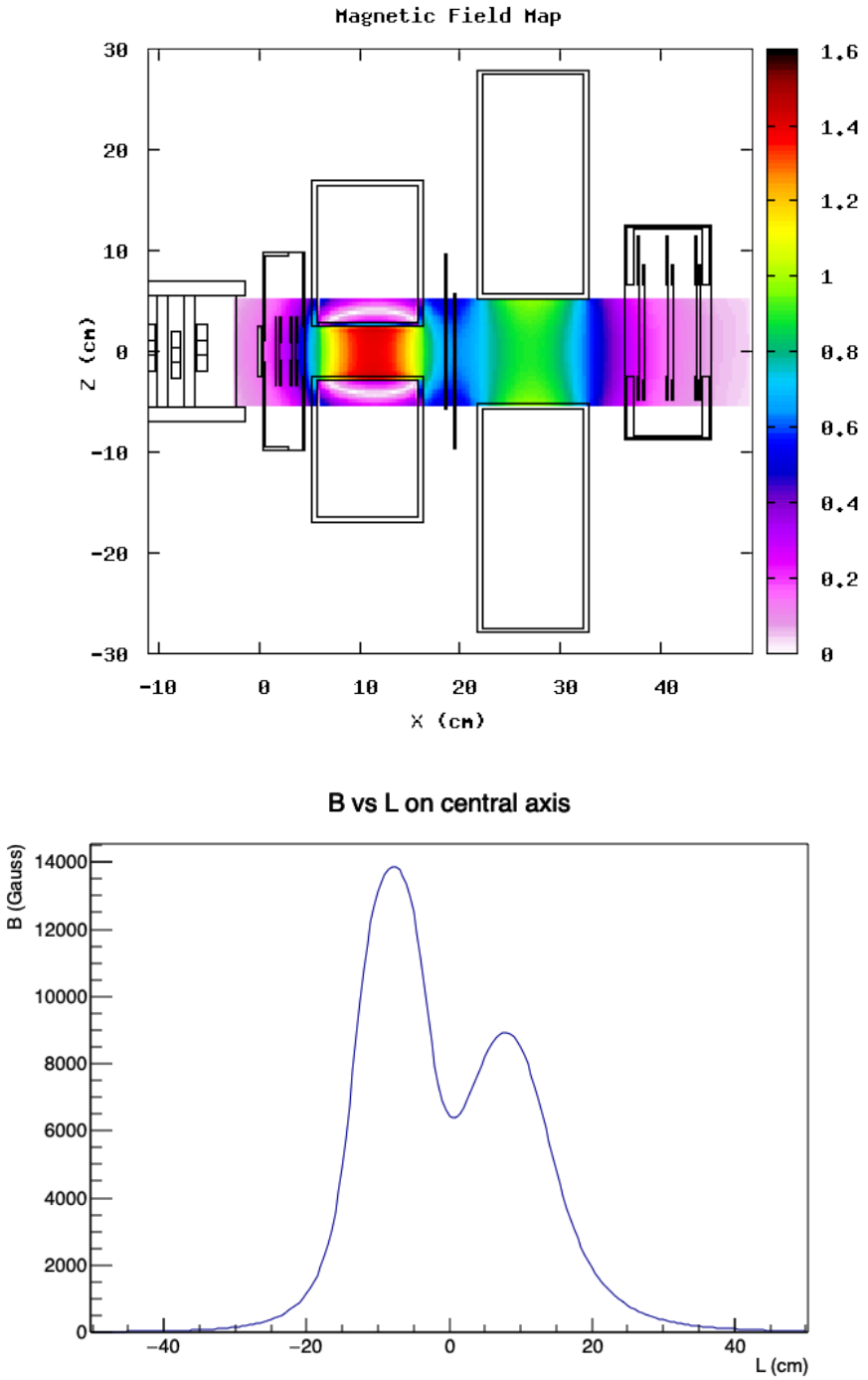

Figure 10: Top panel: color map of the magnetic field intensity in the $z - x$ plane (scale is in Tesla). Bottom panel: module of magnetic field as a function of z coordinate. Here $\vec{B}$ units are in Gauss and $z = 0$ cm is the coordinate of the center of the two magnets system.

For example, the pixel detectors measure the particles position, while the scintillator gives energy release and timing information. Therefore, the output has to be modeled on the detectors characteristics, reproducing the information given by each of them. In addition, in order to allow detailed studies of the interaction processes, it is important to exploit all available MC data to record the whole history of the particles produced in the same event.

FLUKA user routines are called in different moments of the run, *i.e.:* at the beginning/end of the run or of each event, during particle tracing, at interaction points etc. Beyond user routines, auxiliary files are also necessary. For example: include files, the map of the magnetic field, etc. The coding of the user routines necessary for the simulation of the FOOT MS is based on the experience collected in previous experimental situations[19, 32, 33, 34, 35].At present, the user routines and the auxiliary files required to produce the FOOT simulations output are the following:

- `mgdraw.inc`: this is a custom *include* file containing the common blocks shared by the other user routines. In FORTRAN, a common block is a section of memory where data are stored for use across multiple routines, without the need to pass arguments. This file, reporting the common blocks declarations, is not a standard FLUKA routine but has been introduced for programming convenience.

- `parameters.inc`: another custom *include* file containing detectors parameters needed and used by the other user routines. Since these parameters are strictly related to the geometry, this file is automatically generated when producing the FLUKA geometry with the `MakeGeo` macro to reduce the probability of introducing errors.

- `usrini.f`: this file contains the initialization subroutine `USRINI`, which is called at the beginning of the run by the `USRICALL` card in the input file. The meaning of the numerical parameters in this data card is user defined. Therefore the calling parameters can provide the `USRINI` subroutine with useful paramters or flags to drive the routines actions. In the FOOT input, the `USRICALL` card provides two flags: a debug flag producing, if activated, a verbose output, and an event display flag. Since the customized scoring in the detectors is performed on a region basis, the main task of the `USRINI` subroutine is to recognize and store the region names. In fact, each region of the experimental setup has a double identifier: the first one is its name defined and used by the user, while the second one is a sequential number internally assigned and used by FLUKA. Hence, an algorithm capable of linking the region name to the FLUKA internal number has been implemented in the `USRINI` subroutine. This allow the user to easily recall in the other user routines the regions in which the scoring must be performed.

- `usrein.f`: it contains the `USREIN` subroutine, which is called at the beginning of each event before the sampled primary is transported. In FOOT simulations, it allows the user to initialize the event by zeroing the output arrays of the common blocks declared in the `mgdraw.inc` file.

- `mgdraw.f`: the subroutine `MGDRAW` contained in this file is the core of the output building, since it handles the energy depositions recording. It allows to intercept the transport and the interaction processes at every step. This subroutine is activated by the card `USRDUMP`, and it is used to write the output file where all or selected transport events are recorded. Several entry points can be found in this subroutine: `SODRAW`, which manages the injection of the primary particle in each event; `MGDRAW`, in which the customized scoring in the detector regions is coded and the energy deposition along each step is calculated; `BXDRAW`, in which the scoring at region crossings is performed; `ENDRAW`, which handles local depositions of particles below threshold; `USDRAW`, where the simulation searches inelastic nuclear interactions in the target or in other regions of interest

- `UpdateCurrentParticle.f`: this is not a standard FLUKA user routine. It manages the logic to recognize new created particles and is called by the various entries in `mgdraw.f`.

- `mgdraw_lib.f`: this is not a standard FLUKA user routine, but it is a custom service routine for `MGDRAW`. It contains the custom service subroutines that fill the output arrays for every specific detector and for crossing borders.

- `magfld.f`: the subroutine `MAGFLD` is activated by the input card `MGNFIELD`. It returns the magnetic field intensity and direction on the basis of the current position and region. This subroutine is called only if the region where the particle is transported in that moment has a magnetic flag activated in the card `ASSIGNMA`. In FOOT simulation, this routine reads a file containing a magnetic field map and interpolates it at run time when tracking in a region with an activated magnetic field.

- `usreou.f`: the `USREOU` subroutine contained in it is called at the end of each event, *i.e.* when the primary and all its descendant particles have been transported. In FOOT case, this subroutine writes the output arrays on the output ASCII file at the end of the event.

- `usrout.f`: it contains the `USROUT` subroutine, which is called at the end of the run by the card `USROCALL` in the input file. It can be used to print customized output.

Several check-points placed in the user routines can write in the `log` file user defined error messages, if any, thus allowing the user to control the correctness of the run.

The simulation output can be produced by launching the FLUKA run together with the executable generated by linking the properly compiled user routines. During the run each routine will be called at the right time, thus ensuring the correct management of the scoring throughout the entire run.

These routines are designed to generate the simulation output as a temporary ASCII file. In a second stage, the ASCII file is converted into a `ROOT` file In order to produce a simulation output file comparable to the real data format and not related to the FLUKA code. This conversion is accomplished by means of a simple `ROOT` macro.

The customized event-by-event output has been designed with the goal of storing and writing in the output file all the information which allows a complete understanding and reconstruction, in particular space-time coordinates, kinematics and energy depositions in the active detectors ("hits"). This is accomplished by means of data structures, which can be summarized as follows.

- *Particles block.* In this block the number of particles produced in that event is reported as well as some quantities for each particle, such as its type, mass, charge, production position and momentum, etc. In Tab. 1 an overview of the quantities stored in the particle block for each particle in each event is reported. In this and in the following tables, the variables are reported as they are defined in the `ROOT` macro developed to readout the custom ASCII output file of the FLUKA simulation.

- *Detector blocks.* For each event there are several detector blocks, each one corresponding to one of the detectors in the FOOT MS setup. In these blocks the information about the single detectors output and about energy releases are saved. Blocks corresponding to different detectors differ slightly from one to another because, as well as general quantities, they contain also detector specific information, which are usually related to the detector segmentation. As an example, in case of the VT detector, the layer number is provided (Tab. 2). A similar data format exists for MSD. For IT the number of the hit sensor (0–31) is given. In the case of the TW scintillator, in addition to the layer number, the bar number is also given. In

the case of the calorimeter, the crystal number is the relevant variable. Every energy release described in these blocks can be linked to the particle that produced it through a specific pointer variable (for example `VTXid` in case of the VT detector), which link the energy release in the detector block and the responsible particle in the particle block. This allows the user to retrieve all "MC truth" information about that particle.

- *Crossings block*. The last block contains information about the particle that cross different regions of the setup, both active and inactive (Tab. 3). Also in this case, the particle "MC truth" data related to a specific crossing can be retrieved through a specific linking variable as in detector blocks.

Variable name	Meaning
`int fMotherId`	index of the particle parent
`int fCharge`	charge (Z)
`int fBaryon`	barionic number
`int fRegion`	number of the FLUKA region where the particle is born
`int fType`	FLUKA code for the particle
`TVector3 fInitPos`	coordinates of the production position of the particle (cm)
`TVector3 fFinalPos`	coordinate of the death position of the particle (cm)
`TVector3 fInitMom`	components of the momentum of the particle at production point (GeV/c)
`TVector3 fFinalMom`	components of the momentum of the particle at death point
`double fMass`	mass (GeV/c^2)
`double fTime`	production time (s)
`double fTof`	time between death and production (s)
`double fTrkLength`	track length of the particle (cm)

Table 1: The particle block. All these variables are stored for each particle produced in each event.

Variable name	Meaning
`int fTrackId`	pointer position in the particle block to the particle responsible of the hit
`int fLayer`	vertex layer number
`TVector3 fInPosition`	coordinates of the beginning position of the hit (cm)
`TVector3 fOutPosition`	coordinates of the ending position of the hit (cm)
`TVector3 fInMomentum`	momentum components of the particle at the beginning position of the hit (GeV/c)
`TVector3 fOutMomentum`	momentum components of the particle at the ending position of the hit (GeV/c)
`double fDeltaE`	released energy (GeV)
`double fTof`	time at which the hit has been produced (s)

Table 2: Example of detector block: the vertex block.

In order to produce this customized output, several FLUKA user routines have been used. They are described in the following subsection.

At this stage, neither efficiency nor smearing due to the detector response have been introduced. It has been considered as more convenient to add these effects, together with other detector related details (as for example

Variable name	Meaning
`int fID`	pointer position in the particle block to the particle responsible of the crossing
`int fCrossN`	number of the FLUKA region where the current particle is entering
`int fOldCrossN`	number of the FLUKA region from which the current particle is exiting
`TVector3 fPosition`	coordinates of the position of the boundary crossing (cm)
`TVector3 fMomentum`	momentum components of the particle boundary crossing (GeV/c)
`double fMass`	mass of the particle at the crossing (GeV/c^2)
`double fCharge`	charge number of particle at the crossing
`double fTime`	time of the boundary crossing (s)

Table 3: Crossings block. These variables are saved for each particle at each cross of FLUKA region.

pixel clustering in the M28 chips) in the reconstruction software, thanks to the digitizer classes. In this way, the MC simulation file can be used for detector studies, and there is no need to rerun the simulation with each change in detector parameters.

4. Custom geometry generation in FLUKA and ROOT

Within the FOOT experiment, a software framework has been designed to generate the FLUKA input files and geometry, to read both experimental and simulated data, to perform a local and a global track reconstruction procedure and, eventually, to perform the whole cross section data analysis. This framework, denominated SHOE, is based on the software from the FIRST experiment [19]. A future article will describe the FOOT general reconstruction and analysis software. In the following we shall summarize its main features and describe in more details the procedure for the generation of FLUKA input and geometry.

4.1. General overview of the SHOE software

In the first stage, the SHOE software reads the input data and retrieves the configuration, mapping and geometrical parameters of all the detectors involved in a given campaign. Then, in the case of MC simulated data, the first local reconstruction phase consists in the conversion of the MC information into detector related variables through the detector response function. As an example, the VT MC hits are converted into VT clusters with sizes that depend on the particle energy release and the detector response. Then the clusters are fitted according to a VT local tracking algorithm providing the VT tracks for each event. As another example, the measure of the energy release in TW hits combined with the TOF measurement by SC and TW are used to identify the fragment charge (Z) for each track entering in the TW [12]. In this phase, all the detector performance parameters, such as efficiency and spatial-time resolutions, are considered to tailor the simulation output to the experimental scenario. In addition, there is also the possibility of reproducing the noise and the pile-up background adding fake detector hits. In this first stage, all the coordinates and detector related variables are defined in their own local system of reference, where the origin of the axis is placed in the detector centre. Different local track reconstruction algorithms have been developed for the tracking detectors composed of three or more layers of stations (BM, VT, IT and MSD), providing the possibility to reconstruct a primary or fragmented particle track using only the specific detector hits. These tracks are useful for the detector performance assessment studies and for the detector inter-alignment procedures. In case of experimental data,

the raw measurements are elaborated to reconstruct the physics quantities relevant for each detector, creating the same detector related variables as in the MC simulation case. After the local reconstruction phase, a global reconstruction procedure is performed to determine the whole particle track parameters and properties in all the FOOT detectors. In particular, the track reconstruction is performed by means of a Kalman filter FOOT algorithm implemented in the external open source GENFIT library [36], which takes into account magnetic fields and MCS inside crossed materials. In this stage, the tracks are reconstructed in the global system of reference, the one of the laboratory where all the detector are placed or simulated.

The fact that MC and experimental data are converted into the same detector variables ensures the possibility to use exactly the same reconstruction and analysis software for both. Once the MC simulation output is properly tuned on the experimental parameters, the analysis on the reconstruction software and the detector performances can be easily conducted using both MC and experimental data.

4.2. The geometry management

Geometry, materials and magnetic field characterizing the simulated FOOT setup are required not only by FLUKA to produce simulated data, but also by the reconstruction software to evaluate the MCS and reconstruct the hits position. For this reason, the geometry, materials and magnetic field simulated with FLUKA must be identical to the ones used in the reconstruction software in SHOE. However, while the magnetic map file can be easily read from both FLUKA and SHOE, the logic used by FLUKA to describe geometry and materials is completely different from the one adopted in the reconstruction code by GENFIT, which makes use of `ROOT` geometry classes. After an initial phase when all the geometry or simulation parameters changes were implemented by hand, *i.e.* by directly modifying the FLUKA input files, the necessity of writing the input in a more automated way became evident due to the increasing complexity of the geometry. Moreover, to investigate the detector performances, several simulations differing slightly one from another were often required: for example, to study the particle reconstruction performances we tested different setup configurations with the detectors placed at different distances from the target, and therefore each body used to define the regions associated to a certain detector should have been consequently modified to move them in the geometry space. Performing such modifications by hand is impractical, excessively time-consuming and therefore not an efficient method. To overcome this issue and improve the efficiency of the geometry implementation process, new *ad hoc* SHOE classes have been developed. The classes, one for each detector, take care of producing the geometry both in FLUKA and in `ROOT` format. In particular, the geometrical parameters classes read a configuration file specific for each detector and each data acquisition or simulation campaign, containing all the parameters related to the geometry and the material composition. Even if `ROOT` embeds a quite complete pre-built elements database, we preferred to use exactly the same material definitions used in FLUKA to obtain the best possible matching. To this purpose, another class, called `Materials`, have been developed in the SHOE libraries to manage the materials creating the material and mixture objects which are required by SHOE and storing the information for the `MATERIAL` and the `COMPOUND` cards adopted in FLUKA. Two separated methods create the `ROOT` volume objects and the FLUKA `BODY`, `REGION`, `MATERIAL`/`COMPOSITION` and `ASSIGNMA` cards to create each detector volume with the appropriate material composition in their local reference system. Even if the two methods are separated, they are forced to read the same detector geometrical parameters from the same `parGeo` classes, minimizing the possibility of having potential mismatches between the two geometries. Then, all the detector `ROOT` objects are collected by the SHOE global geometry manager which is responsible for placing all

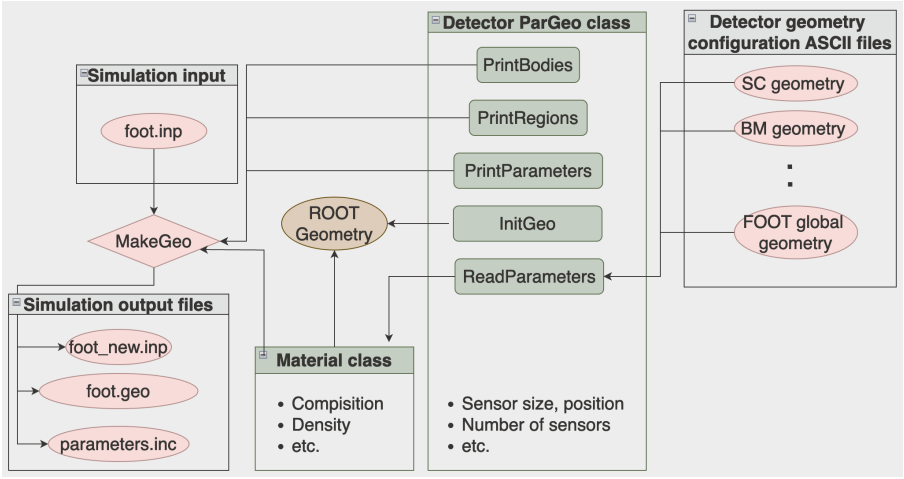

Figure 11: Simplified scheme of the SHOE software geometry management.

the detectors in the right spatial position, creating the whole apparatus volume for `ROOT` and `GENFIT` framework. Also in this case, the positions and the rotations of the detectors are read from an external configuration file handled by a dedicated class. A scheme of the geometry management of the SHOE software is shown in Fig. 11 The advantage of using external configuration files is that it allows not only to adjust the position and tilt of the detectors, which may vary across the campaigns, but also to create geometries that are quite different from each other by simply changing a few parameters while keeping the core unchanged. As an example, the simulation of a new VT detector with a different number of layers, different size and different pixel pitch can be created just modifying three parameters. Considering also the possibility to exploit the same reconstruction and analysis code, the detector upgrade studies can be conducted smoothly and efficiently. During an experimental data-taking campaign, this geometry management system allows for easy and rapid reproduction of the experimental composition and geometrical positioning of the detectors in a MC simulation, ensuring the ability to quickly generate simulation output for preliminary data analysis tasks.

4.3. The MakeGeo software

Different methods have been developed to handle the FLUKA simulation input files within the `parGeo` classes, similar to the methods developed to create and manage the `ROOT` geometry. In the SHOE software, as shown in Fig. 11, a specific executable `MakeGeo` reads a FOOT reference input file (`foot.inp`) and creates, as output, the new input file (`foot_new.inp`) with a the geometrical parameters written in a separated file (`foot_new.geo`) and a parameter file used by the FLUKA ROUTINES to run the simulation (`parameters.inc`). The new input file copies the fixed simulation cards from the old `foot.inp` file (e.g.: `PHYSICS` cards) and modifies the simulation campaign related parameters (e.g.: `BEAM` cards). Instead, the FOOT geometry file is written by calling from each detector `parGeo` class the methods `PrintBodies`, `PrintRegions` and `PrintParameters`, which implement the logic to write the FLUKA *bodies* and `REGION` cards in the `foot.geo` file. The transformation from the local to the global system of reference is achieved using the `ROT-DEFINI` cards defined by each detector.

5. Simulation Performance

MC simulation is essential in the experiment for several purposes. The first important task is the prediction of expected physics results, which are of course affected by the unavoidable uncertainties of the physics models

of the code. The purpose of the FOOT experiment is exactly to provide data useful for the improvement of such models. However, data collected in previous experiments at energies close to the range explored by FOOT[37, 18, 38, 39] allowed to estimate that the shape of both angular and energy distribution of secondary fragments, as generated by FLUKA, have an uncertainty level which allow to achieve a conservative design of the experiment. This assertion is also quantitatively supported by the first preliminary results of FOOT, obtained in a test performed using a partial setup of the apparatus which consisted only of the FOOT TOF-ΔE system (SC+TW) and BM [40]. In this test was possible to measure the elemental cross sections for the production of different nuclear fragments, selected in the energy range 100-600 MeV/u and $0 \leq \theta \leq 5.7°$, in the interactions of ^{16}O projectiles at 400 MeV/u on a graphite target. The comparison of measured cross sections with FLUKA predictions is reported in Tab.4.

Element	$\sigma_{exp} \pm \Delta_{stat} \pm \Delta_{sys}$ [mbarn]	σ_{MC} [mbarn]
He	789 ± 35 ± 67	705.0
Li	101 ± 13 ± 10	74.9
Be	33 ± 9 ± 3	37.5
B	78 ± 11 ± 6	41.8
C	131 ± 14 ± 4	87.7
N	117 ± 14 ± 6	110.3

Table 4: Measured elemental fragmentation cross sections, selected in the energy interval 100-600 MeV/u and $0 \leq \theta \leq 5.7°$, for a 400 MeV/u ^{16}O beam interacting with a 5 mm graphite target as compared with FLUKA MC predictions[40]

In Fig.12 an example of a simulated nuclear multi-fragmentation event is shown, where charged particles tracks are drawn in a 3 dimensional rendering of the simulated geometry. They have been obtained from the simulation of the interaction of ^{12}C ions at 200 MeV/u against a graphite target.

Monte Carlo simulation is then fundamental in different stages of data analysis. The accurate and detailed reproduction of detector geometry allows to evaluate geometrical acceptance. The simulation of detector response, obtained by folding the MC output with the resolution features of the single elements, as experimentally determined in test beams, combined with the geometrical acceptance, allows to evaluate the efficiency for all specific reaction channels investigated by the experiment, so to make possible the extraction of cross sections.

In some aspects, MC is also used in the procedures for detector calibration. In the FOOT experiment, one of the most important cases is the calibration of the response of the TW scintillators, so to achieve the correct Z-identification[12]. An example of the quality of the calibration results is given by Fig.13, where the energy release in the TW for different charged fragments in experimental and MC data are compared. Experimental data have been collected from a run using a ^{12}C primary beam at 200 MeV/u against a graphite target. The experimentally determined time and energy resolutions have been folded with the MC expectations.

The accurate reproduction of material properties helps to evaluate the possible background. The possible sources are many. Among them, the out-of-target interaction of primary particles, or the re-interaction of secondary fragments.

Last but not least, since our Monte Carlo simulation is capable of produce an output in the same format as that of experimental data, the development, test and training of track reconstruction software has been possible.

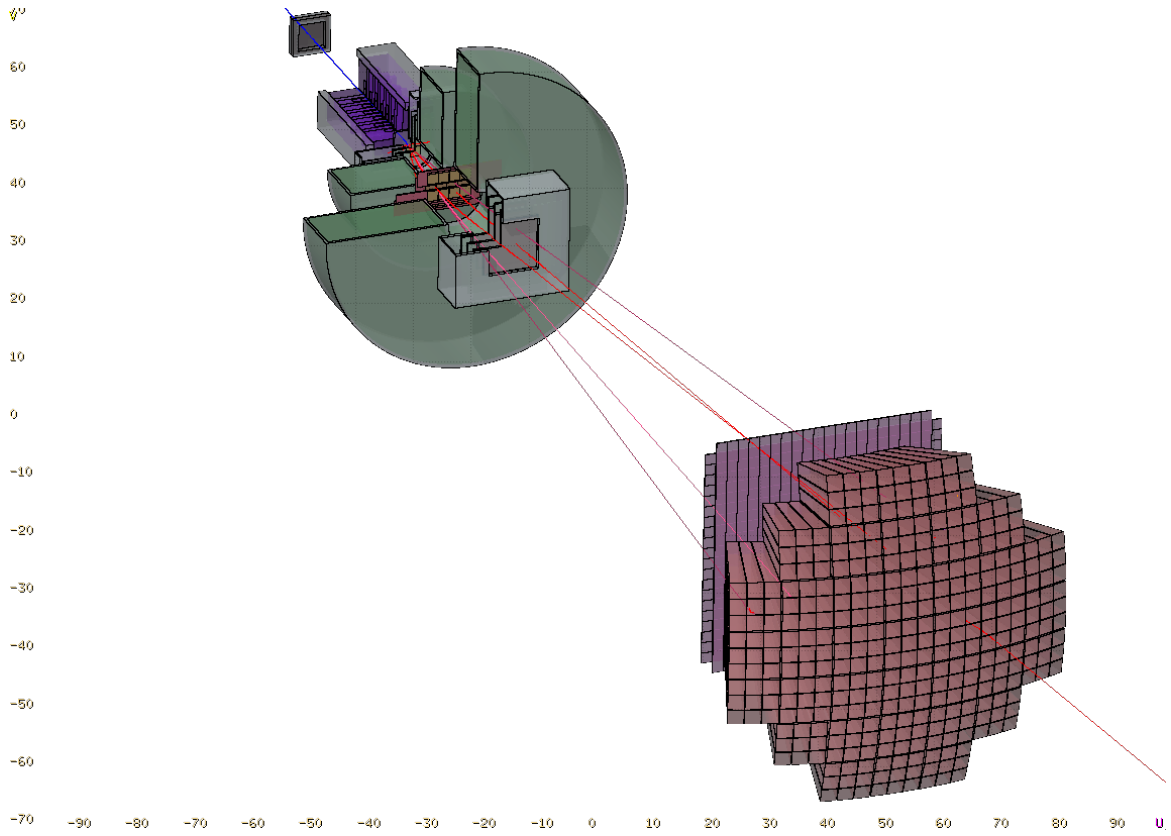

Figure 12: Example of simulated event: ^{12}C projectiles at 200 MeV/u onto a graphite target, producing several charged fragments. Different colours represent different particles or nuclear fragments. Neutrons, e^+, e^- and photons are not shown.

In this way it was possible to evaluate mis-reconstruction probabilities and evaluate many factors contributing to systematic uncertainties associated to data reconstruction.

5.1. Time and memory usage

In Tab. 5 the CPU time per event and the size of both the ASCII and the ROOT output files are reported for different primaries and energies. The 2024.1.0 version of FLUKA was used, on a single core of i7-8700K CPU, 3.7 GHz. The ROOT file size is about $20 - 24\%$ of the ASCII file size due to the compression algorithm. The computation time and disk space difference between the cases of carbon ion and oxygen primary beams is almost negligible. Instead, there is a clear correlation both for the computation time and disk space with varying primary energy. As expected, increasing the projectile energy led to a higher number of nuclear interactions and, consequently, to an increased number of simulated particles. The majority of hadrons ($\gtrsim 50\%$) are created in the calorimeter: actually, it behaves as a primary beam dump. Instead, the mean number of hadrons per event produced in a 5 mm thick graphite target ($0.915\, g/cm^2$) is about $0.4 - 0.5$. This mean includes the cases in which no fragments has been produced in the target. The percentage of carbon ions interacting in the target is between 3.2 and 3.7%, depending on the energy, while for the case of oxygen ions this percentage rises to the 4.2-5.1% interval.

The possible use of low energy thresholds for e^+,e^- when, for instance, δ-ray production is needed, can significantly slow down the simulation speed. For example, a cut-off at 100 keV for electrons, increases the average CPU time by about one order of magnitude and produces an output file larger by a factor of $\sim$5.

To evaluate detector performances a minimum reasonable number of simulated primaries is about 1×10^7. The FLUKA management of the seeds of random number sequence directly from the input file allows to easily

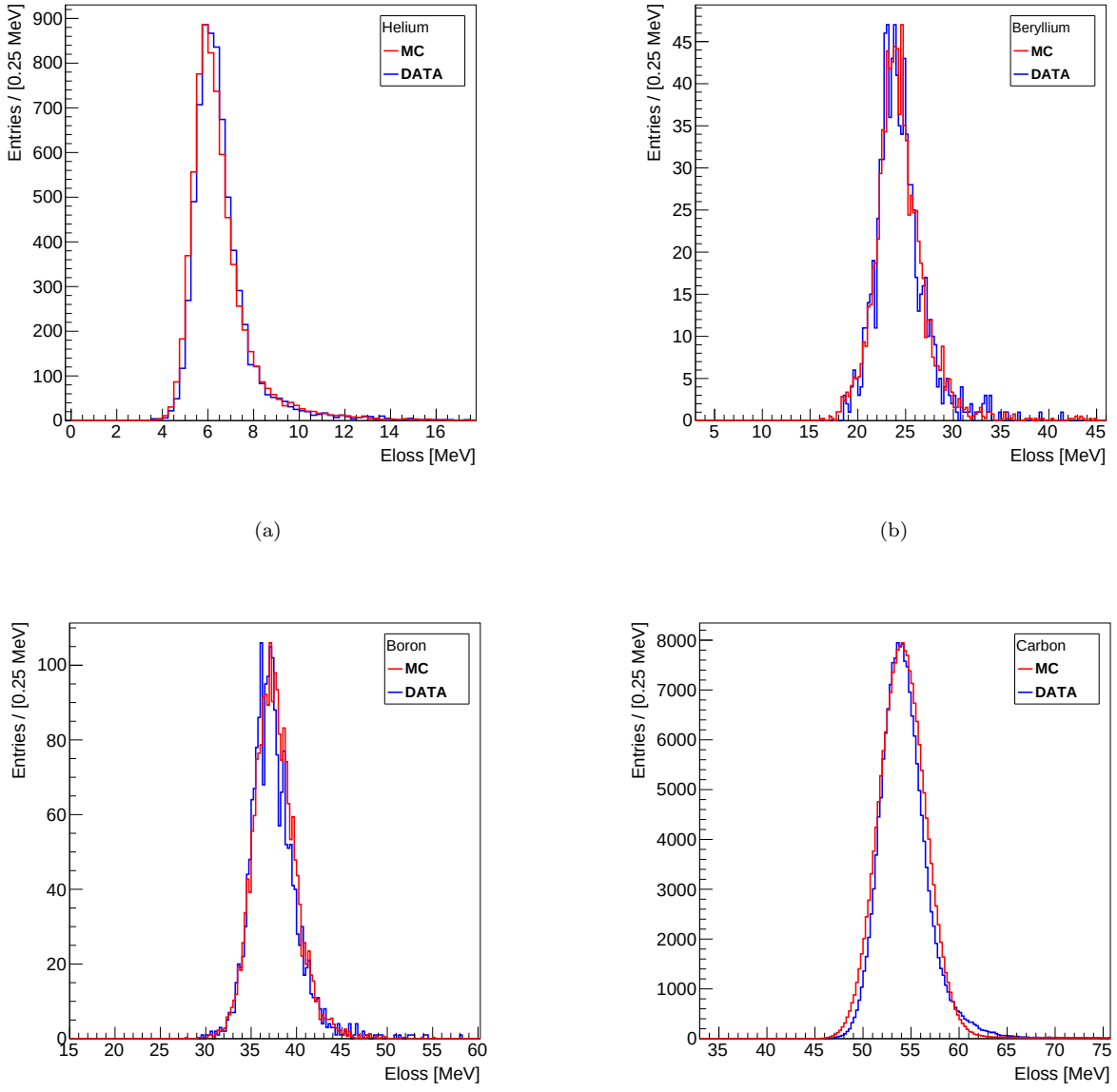

(a) (b)

(c) (d)

Figure 13: Comparison of predicted (red histograms) and measured (blue histograms) energy loss distribution in the TofWall detector of FOOT experiment for different charged fragments produced in the collisions of ^{12}C ions at 200 MeV/u on a graphite target: Z=2 (a); Z=4 (b); Z=5 (c); Z=6 (d). The Z=6 plot is populated mostly by non-fragmented primaries. The experimentally evaluated resolutions have been folded with the simulation and distributions have been normalized to the peak value.

Projectile	Primary Energy [200 MeV/u]	Average CPU time [msec/primary]	ASCII file size [Mb]	ROOT file size [Mb]	<hadrons>/event
^{12}C	200	64.29	3472	811	8.2
^{12}C	400	83.40	13819	2927	39.5
^{12}C	700	131.2	35187	7304	103.9
^{16}O	200	64.28	3315	779	7.9
^{16}O	400	88.09	13997	2964	40.9
^{16}O	700	143.4	39111	8106	115.8

Table 5: Examples of time and memory usage for simulations with samples of 5×10^4 primaries conducted on a Intel i7-8700K CPU, x86_64, 3.70GHz.

split the production in many statistically independent jobs, to be run in parallel using different CPU cores. We do not make use of any biasing technique among those available in FLUKA, otherwise this would be incompatible with the goal of achieving an event-by-event output capable of reproducing all statistical moments of experimental distributions.

6. Discussion and Conclusions

In this work we have described the organization and the performance of the FLUKA simulation of the electromagnetic setup of the FOOT experiment. The optimization of the procedure and of the customized event-by-event output is the result of the expertise gained after several experiments carried out in applied nuclear physics at intermediate energies for more than ten years. In particular, the structure of the output file allows to reconstruct the whole history of each event, and this feature turns out to be a powerful tool for the comprehension of the detector response and efficiency, of background generation and of the involved physics processes as well. On the other hand, this kind of output becomes unpractical when the number of particles, including those generated in secondary interactions, becomes too large. Therefore this system has to be limited to primary energies not larger than 1 GeV/u. However, from a general point of view, the custom event output structure developed for this activity, although not standard, turned out to be a very powerful tool at the energies of interest for the FOOT experiment. It can be easily implemented in the FLUKA simulation of any experiment operating in the same range of energy.

From the point of view of workflow management, the adopted approach, which integrates the simulation into the overall software framework of the experiment, allows to achieve a very powerful and flexible system. It permits to rely upon the geometrical survey of the apparatus in a given experimental campaign, assuring a common reference for both simulation and data reconstruction software. This feature is of particular importance for the FOOT experiment, since, not being a fixed installation, it has to be moved and re-installed in different experimental sites and environmental conditions. In addition, such a unique framework for simulation and reconstruction, allows to use the same software for the analysis of both real and simulated data. This turns out to be fundamental for an efficient development and training of the algorithms to be used in the physics analysis of the FOOT experiment.

A discussion on the features and quality of the physics models of the FLUKA Monte Carlo code is instead outside the scope of this work. Actually, the FOOT experiment has been designed exactly for the purpose of measuring single and double differential cross sections in energy regions in which Monte Carlo models are

affected by important systematic uncertainties. Therefore, also the FLUKA models will be hopefully improved, if needed, by the results eventually achieved by the FOOT experiment.

Acknowledgments

We wish to thank the FLUKA authors, and in particular A. Ferrari and P.R. Sala, for providing several advices and explanations.

References

[1] Tommasino, F., Durante, M.. Proton radiobiology. Cancers 2015;7(1):353–381.

[2] Durante, M., Paganetti, H.. Nuclear physics in particle therapy: a review. Reports on Progress in Physics 2016;79(9):096702.

[3] Embriaco, A., Attili, A., Bellinzona, E., Dong, Y., Grzanka, L., Mattei, I., et al. Fluka simulation of target fragmentation in proton therapy. Physica Medica 2020;80:342–346.

[4] Bellinzona, E., Grzanka, L., Attili, A., Tommasino, F., Friedrich, T., Krämer, M., et al. Biological impact of target fragments on proton treatment plans: An analysis based on the current cross-section data and a full mixed field approach. Cancers 2021;13:4768.

[5] Norbury, J., et al. Review of nuclear physics experiments for space radiation. 2011. NASA/TP-2011-217179.

[6] Slaba, T.C., Blattnig, S.. Gcr environmental models i: Sensitivity analysis for gcr environments. Space Weather 2014;12:217–224.

[7] Zeitlin, C., La Tessa, C.. The role of nuclear fragmentation in particle therapy and space radiation protection. Frontiers in Oncology 2016;6:65.

[8] Norbury, J., Battistoni, G., Besuglow, J., Bocchini, L., Boscolo, D., Botvina, A., et al. Are further cross section measurements necessary for space radiation protection or ion therapy applications? helium projectiles. Frontiers in Physics 2020;8:565954.

[9] Parodi, K., Mairani, A., Brons, S., Hasch, B., Sommerer, F., Naumann, J., et al. Monte Carlo simulations to support start-up and treatment planning of scanned proton and carbon ion therapy at a synchrotron-based facility. Phys Med Biol 2012;57(12):3759.

[10] Grassberger, C., Daartz, J., Dowdell, S., Ruggieri, T., Sharp, G., Paganetti, H.. Quantification of proton dose calculation accuracy in the lung. Int J Radiat Oncol Biol Phys 2014;89(2):424–30.

[11] Muraro, S., Battistoni, G., Kraan, A.C.. Challenges in monte carlo simulations as clinical and research tool in particle therapy: A review. Frontiers in Physics 2020;8:567800.

[12] Battistoni, G., Toppi, M., Patera, V., and the FOOT Collaboration, . Measuring the impact of nuclear interaction in particle therapy and in radio protection in space: the FOOT experiment. Frontiers in Physics 2021;8:568242.

[13] Ferrari, A., Sala, P.R., Fasso, A., Ranft, J.. FLUKA: A multi-particle transport code (Program version 2005). Tech. Rep. CERN-2005-010, SLAC-R-773, INFN-TC-05-11, CERN-2005-10; CERN INFN SLAC; 2005.

[14] Böhlen, T., Cerutti, F., Chin, M., Fassò, A., Ferrari, A., Ortega, P.G., et al. The fluka code: developments and challenges for high energy and medical applications. Nuclear data sheets 2014;120:211–214.

[15] Battistoni, G., Boehlen, T., Cerutti, F., Chin, P.W., Esposito, L.S., Fassò, A., et al. Overview of the fluka code. Ann Nucl Energy 2015;82:10–18.

[16] Battistoni, G., Bauer, J., Boehlen, T.T., Cerutti, F., Chin, M.P.W., Augusto, R.D.S., et al. The FLUKA code: an accurate simulation tool for particle therapy. Frontiers in oncology 2016;6:116.

[17] Mattei, I., Alexandrov, A., Alunni Solestizi, L., Ambrosi, G., Argirò, S., Bartosik, N., et al. Measurement of 12c fragmentation cross sections on c, o, and h in the energy range of interest for particle therapy applications. IEEE Transactions on Radiation and Plasma Medical Sciences 2020;4(2):269–282. doi:10.1109/TRPMS.2020.2972197.

[18] Divay, C., Colin, J., Cussol, D., Finck, C., Karakaya, Y., Labalme, M., et al. Differential cross section measurements for hadron therapy: 50 MeV/nucleon ^{12}C reactions on H, C, O, Al, and Ti targets. Phys Rev C 2017;95:044602.

[19] Pleskac, R., Abou-Haidar, Z., Agodi, C., Alvarez, M.A.G., Aumann, T., Battistoni, G., et al. The FIRST experiment at GSI. Nucl Instrum Meth A 2012;678:130–138.

[20] Dong, Y., Silvestre, G., Colombi, S., Alexandrov, A., Alpat, B., Ambrosi, G., et al. The drift chamber detector of the foot experiment: Performance analysis and external calibration. Nuclear Instruments and Methods in Physics Research Section A: Accelerators, Spectrometers, Detectors and Associated Equipment 2021;986:164756.

[21] Kraan, A., Zarrella, R., Alexandrov, A., Alpat, B., Ambrosi, G., Argirò, S., et al. Charge identification of nuclear fragments with the foot time-of-flight system. Nuclear Instruments and Methods in Physics Research Section A: Accelerators, Spectrometers, Detectors and Associated Equipment 2021;1001:165206. doi:https://doi.org/10.1016/j.nima.2021.165206.

[22] Fassò, A., Ferrari, A., Ranft, J., Sala, P.. New developments in fluka modelling of hadronic and em interactions. In: KEK Proceedings; vol. 97. National Laboratory for High Energy Physics; 2007, p. 32–43.

[23] Böhlen, T., et al. Benchmarking nuclear models of FLUKA and GEANT4 for carbon ion therapy. Phys Med Biol 2010;55(19):5833.

[24] Cerutti, F., Battistoni, G., Capezzali, G., Colleoni, P., Ferrari, A., Gadioli, E., et al. Low energy nucleus–nucleus reactions: the bme approach and its interface with fluka. In: Proc. 11th Int. Conf. Nuclear Reaction Mechanisms; vol. 126. 2006, p. 507–514.

[25] Cerutti, F., Empl, A., Fedynitch, A., Ferrari, A., Ruben, G., Sala, P.R., et al. Nuclear model developments in fluka for present and future applications. In: EPJ Web of Conferences; vol. 146. EDP Sciences; 2017, p. 12005.

[26] Ballarini, F., Battistoni, G., Belcari, N., Bisogni, G., Campanella, M., Carante, M., et al. FLUKA: status and perspectives. In: 15th Workshop on Shielding Aspects of Accelerators, Targets, and Irradiation Facilities" (SATIF15). 2022,.

[27] Andersen, V., Ballarini, F., Battistoni, G., Campanella, M., Carboni, M., Cerutti, F., et al. The fluka code for space applications: recent developments. Adv Space Res 2004;34(6):1302–1310.

[28] Sorge, H., Stöcker, H., Greiner, W.. Poincaré invariant hamiltonian dynamics: modelling multi-hadronic interactions in a phase space approach. Ann Phys-New York 1989;192(2):266–306.

[29] Sorge, H.. Flavor production in pb (160a gev) on pb collisions: Effect of color ropes and hadronic rescattering. Phys Rev C 1995;52(6):3291.

[30] Reidel, C.A., Schuy, C., Finck, C., Horst, F., Boscolo, D., Baudot, J., et al. Response of the mimosa-28 pixel sensor to a wide range of ion species and energies. Nuclear Instruments and Methods in Physics Research Section A: Accelerators, Spectrometers, Detectors and Associated Equipment 2021;1017:165807. URL: https://www.sciencedirect.com/science/article/pii/S0168900221007920. doi:https://doi.org/10.1016/j.nima.2021.165807.

[31] ???? OPERA magnetic modelling software, Cobham (Vector Fields), http://www.cobham.com/.

[32] Agodi, C., Battistoni, G., Bellini, F., Cirrone, G.A.P., Collamati, F., Cuttone, G., et al. Charged particle's flux measurement from PMMA irradiated by 80 MeV/u carbon ion beam. Phys Med Biol 2012;57(18):5667.

[33] Agodi, C., Battistoni, G., Bellini, F., Cirrone, G.A.P., Collamati, F., Cuttone, G., et al. Charged particles flux measurement from PMMA irradiated by 80 MeV u($^{-1}$) carbon ion beam. Physiscs in Medicine and Biology 2014;59(23):7563–7564.

[34] Piersanti, L., Bellini, F., Bini, F., Collamati, F., De Lucia, E., Durante, M., et al. Measurement of charged particle yields from PMMA irradiated by a 220 MeV/u ^{12}C beam. Physincs in Medicine and Biology 2014;59(7):1857.

[35] Rucinski, A., Battistoni, G., Collamati, F., De Lucia, E., Faccini, R., Frallicciardi, P.M., et al. Secondary radiation measurements for particle therapy applications: charged particles produced by He-4 and C-12 ion beams in a PMMA target at large angle. Physiscs in Medicine and Biology 2018;63(5).

[36] Rauch, J., Schlüter, T.. GENFIT – a Generic Track-Fitting Toolkit. In: J. Phys. Conf. Ser.; vol. 608. 2015, p. 012042.

[37] Dudouet, J., Juliani, D., Labalme, M., Cussol, D., Angélique, J., Braunn, B., et al. Double-differential fragmentation cross-section measurements of 95 MeV/nucleon ^{12}C beams on thin targets for hadron therapy. Phys Rev C 2013;88:024606.

[38] Toppi, M., Abou-Haidar, Z., Agodi, C., Alvarez, M.A.G., Aumann, T., Balestra, F., et al. Measurement of fragmentation cross sections of ^{12}C ions on a thin gold target with the FIRST apparatus. Phys Rev C 2016;93(6):064601.

[39] Mattei, I., Alexandrov, A., Solestizi, L.A., Ambrosi, G., Argiro, S., Bartosik, N., et al. Measurement of ^{12}C fragmentation cross sections on C, O, and H in the energy range of interest for particle therapy applications. IEEE TRANSACTIONS ON RADIATION AND PLASMA MEDICAL SCIENCES 2020;4(2):269.

[40] Toppi, M., Sarti, A., Alexandrov, A., Alpat, B., Ambrosi, G., Argirò, S., et al. Elemental fragmentation cross sections for a 16O beam of 400 MeV/u kinetic energy interacting with a graphite target using the FOOT ΔE-TOF detectors. Frontiers in Physics 2022;10:979229.